

# Evolutionary Optimization of Dynamic Multi-objective Test Functions

Jörn Mehnert<sup>1</sup>, Tobias Wagner<sup>1</sup>, and Günter Rudolph<sup>2</sup>

<sup>1</sup> ISF, Institut für Spanende Fertigung  
University of Dortmund, Department of Machining Technology  
Baroper Str. 301, 44227 Dortmund, Germany  
{mehnen, wagner}@isf.de, <http://www.isf.de>

<sup>2</sup> LS XI, Chair of Algorithm Engineering  
University of Dortmund, Department of Computer Science  
Otto-Hahn-Str. 14, 44227 Dortmund, Germany  
guenter.rudolph@cs.uni-dortmund.de,  
<http://ls11-www.cs.uni-dortmund.de>

**Abstract.** Multi-objective as well as dynamic characteristics appear in many real-world problems. In order to use multi-objective evolutionary optimization algorithms (MOEA) efficiently, a systematic analysis of the algorithms' behavior in dynamic environments by means of dynamic test functions is necessary. These functions can be classified into problems with changing Pareto sets and/or Pareto fronts with different dynamic criteria. Thus, a test suite with existing benchmark functions having dynamic behavior and new designed dynamic test functions for yet uncovered cases is proposed. Convergence and solution distribution features of modern MOEA, namely NSGA-II, SPEA2, and MSOPS using different variation operators (Simulated Binary Crossover with Polynomial Mutation and Differential Evolution) will be analyzed. For this reason, a new path integral metric is introduced. Especially the transfer of single-objective results and the ability of the algorithms to use historically evolved population properties will be discussed.

## 1 Introduction

An effective optimization of dynamic multi-objective problems using population based optimization algorithms requires a systematic case study. New generic functions are needed to analyze the distribution and convergence properties of MOEA when dynamically varying Pareto front structures or changing restrictions are used. Simple dynamic test functions allow an isolated study of dynamic criteria. Thus, such test functions are developed and empirically analyzed. An insight into this field is given and problems while using standard MOEA in dynamic environments are shown. The application of an open source library (PISA) allows the adaptation of the results to real-world problems and comparability of results.

## 2 Literature on Dynamic Multi-objective Optimization

Dynamic multi-objective function optimization is rarely discussed in current literature. Jin and Sendhoff [1] introduced an open scheme for generating test functions when shifting dynamically between static functions. This approach does not led to clearly defined problems yet. Farina, Deb, and Amato [2, 3] designed dynamic functions following the concepts of Deb et al. [4, 5]. These are currently the only dynamic multi-objective test functions at hand.

To guarantee a comprehensive test suite and an organized analysis of MOEA on dynamic test functions a categorization of used functions is essential. Two different approaches are suggested by Branke [6, page 14 et sqq.] and Farina, Deb, and Amato [2, 3]. The latter classifies dynamics of multi-objective problems into four classes depending on the concerned space:

1. Static Pareto front  $\mathbf{PF}_{true}$ , dynamic Pareto set  $\mathbf{P}_{true}$ ,
2. Dynamic  $\mathbf{PF}_{true}$ , dynamic  $\mathbf{P}_{true}$ ,
3. Dynamic  $\mathbf{PF}_{true}$ , static  $\mathbf{P}_{true}$ , and
4. Static  $\mathbf{PF}_{true}$ , static  $\mathbf{P}_{true}$ . The fitness topology may change.

The dynamics can further be divided into subclasses that correspond to the dynamics in shape or structure (e.g. connectivity) of the Pareto fronts. None, static or dynamic definitions of the feasible set  $\mathbf{D}$  and restrictions in objective space lead to further items usable for a more specified subdivision. As categorized by Branke, different dynamic criteria like frequency, severity, predictability, and cycle length of change have to be taken into account within every class.

In this paper the functions of Farina, Deb, and Amato – called FDA1 to FDA5 – are used as test cases with known properties<sup>3</sup>. They are representatives of the first three classes described and also allow to analyze the effect of Branke’s criteria. The original FDA2 function representing the third class had to be redesigned in order to get a Pareto front that is changing from a convex to a concave shape independent of the decision variables’ assignment. Thus, in the experiments  $FDA2_{mod}$  was used:

$$FDA2_{mod} : \begin{cases} f_1(\mathbf{x}_I) & = x_1 \\ f_2(g, h) & = g \cdot h(f, g) \\ g(\mathbf{x}_{II}, \mathbf{x}_{III}) & = 1 + \sum_{x_i \in \mathbf{x}_{II}} x_i^2 + \sum_{x_i \in \mathbf{x}_{III}} (x_i + 1)^2 \\ h(f_1, g) & = 1 - \left(\frac{f_1}{g}\right)^{H(t(\tau))} \\ H(t) & = 0.2 + 4.8t(\tau)^2 \\ t(\tau) & = \frac{1}{n_t} \left\lfloor \frac{\tau}{\tau_t} \right\rfloor, \tau \text{ current generation} \\ & \tau_t \text{ change rate} \\ & n_t \text{ number of distinct steps} \\ \mathbf{x}_I & = (x_1)^T, x_1 \in [0, 1] \\ \mathbf{x}_{II} & = (x_2, \dots, x_{r_1})^T \in [-1, 1]^{r_1-1} \\ \mathbf{x}_{III} & = (x_{r_1+1}, \dots, x_n)^T \in [-1, 1]^{n-r_1-1} \end{cases} \quad (1)$$

<sup>3</sup> For an explicit definition of the FDA functions please refer to [2, 3].

The change rate  $\tau_t$  is the number of generations for which  $t(\tau)$  remains fixed. Thus,  $\tau_t^{-1}$  describes the frequency of change. The severity of change depends on choice of  $n_t$ . Time  $t$  is restricted to the interval  $[0, 1]$  and the exponent  $H(t)$  is in  $[\frac{1}{5}, 5]$ . In the following the authors use the abbreviation  $t := t(\tau)$ . To guarantee a change from a convex to a concave shape ( $H(t) \geq 1$ ) for  $t \approx 0.5$  the square of  $t$  is calculated.

### 3 New Dynamic Multi-objective Test Functions

The DTLZ and ZDT test functions [4, 5] used as source of the above dynamic functions are already challenging in their static version. To analyze the effect of the different dynamic criteria in a more isolated way, simpler test functions are needed. The new functions *DSW1* to *DSW3* are motivated by the static multi-objective function of Schaffer [7]. The parabolic character of this function shows analogies to the single-objective unimodal sphere model which is used as a typical test case for the analysis in dynamic single-objective continuous optimization [8]. Therefore, the DSW functions allow to compare the results of the MOEA to ones of dynamic single-objective optimization as in literature described. The general scheme used for the DSW functions is

$$DSW : \begin{cases} f_1(\mathbf{x}) = (a_{11}x_1 + a_{12}|x_1| - b_1 \cdot G(t))^2 + \sum_{i=2}^n x_i^2 \\ f_2(\mathbf{x}) = (a_{21}x_1 + a_{22}|x_1| - b_2 \cdot G(t) - 2)^2 + \sum_{i=2}^n x_i^2 \end{cases} \quad (2)$$

where  $G(t) : \mathbb{R} \rightarrow \mathbb{R}$  is a continuous function with monotonously increasing or periodically changing values. The definition  $G(t) := t(\tau) \cdot s$  with  $t(\tau) = \lfloor \frac{\tau}{\tau_T} \rfloor$  is used where  $s$  is the severity of change. If the border of feasible space is reached the shift of  $G(t)$  turns its direction, i.e.  $G(t)$  decreases. In the analysis, the *DSW* functions have been defined as follows:

$$\begin{aligned} DSW1 : \mathbf{x} &\in [-50, 50]^n, a_{11} = 1, a_{12} = 0, a_{21} = 1, a_{22} = 0, b_1 = 1, b_2 = 1 \\ DSW2 : \mathbf{x} &\in [-50, 50]^n, a_{11} = 0, a_{12} = 1, a_{21} = 0, a_{22} = 1, b_1 = 1, b_2 = 1 \\ DSW3 : \mathbf{x} &\in [-50, 50]^n, a_{11} = 1, a_{12} = 0, a_{21} = 1, a_{22} = 0, b_1 = 0, b_2 = 1 \end{aligned}$$

*DSW1* is a test function with static  $\mathbf{PF}_{true}$  ( $f_2^* = (\sqrt{(f_1^*)} - 2)^2$ ) and shifting  $\mathbf{P}_{true}$ . The challenge presented to the MOEA is to keep the value of the first decision variable in the interval  $[G(t), G(t) + 2]$ . This is equivalent to the single-dimensional and single-objective dynamic sphere model where the center of the sphere is shifted with linear speed.

The *DSW2* problem has the two separated Pareto sets which depart diametrically.  $\mathbf{PF}_{true}$  does not change in time and is identical to *DSW1*. With  $n = 1$  the Pareto set is  $\mathbf{P}_{true} = [-G(t) - 2, -G(t)] \cup [G(t), G(t) + 2]$ . For periodical  $G(t)$  the Pareto sets will join and depart periodically.

In problem *DSW3* the right border of the interval of the Pareto set is moving while the other border remains static. This is realized by setting  $b_1 = 0$ . The Pareto set and the corresponding convex Pareto front extend with increasing  $t$ .

The new generic scheme *DTF* is an enhanced generalization of the *FDA* functions and allows a variable scaling of the dynamic properties' complexity. The number  $\psi$  of separated Pareto front sections and the number  $\omega$  of local optimal fronts are introduced, motivated by static test functions ZDT3 and ZDT4 [4]. The curvature of the Pareto front  $\alpha$ , the density of arguments  $\beta$ , and the optimal argument value  $\gamma$  for all  $\mathbf{x}_{II}$  can be adjusted analog to FDA problems.

$$DTF : \begin{cases} f_1(\mathbf{x}_I) = x_1^{\beta(t)} \\ f_2(g, h) = g \cdot h(f, g) \\ g(\mathbf{x}_{II}) = 1 + \sum_{x_i \in \mathbf{x}_{II}} ((x_i - \gamma(t))^2 - \cos(\omega(t)(\tau)) \cdot \pi \cdot (x_i - \gamma(t))) + 1 \\ h(f_1, g) = 2 - \left(\frac{f_1}{g}\right)^{\alpha(t)} - \left(\frac{f_1}{g}\right) \cdot |\sin(\psi(t)\pi f_1)|^{\alpha(t)} \\ \mathbf{x}_I = (x_1)^T, x_1 \in [0, 1] \\ \mathbf{x}_{II} = (x_2, \dots, x_n)^T \in [-1, 1]^{n-1} \end{cases} \quad (3)$$

A typical definition are e.g.  $n = 20$ ,  $\alpha(t) = 0.2 + 4.8t^2$ ,  $\beta(t) = 10^{2\sin(0.5\pi t)}$ ,  $\gamma(t) = \sin(0.5\pi t)$ ,  $\psi(t) = t \cdot s$ ,  $s \in \mathbb{R}_+$ , and  $\omega(t) \propto \psi(t)$ .

In practical applications restrictions cause severe difficulties in optimization problems. The introduction of dynamic restrictions is also motivated by the idea to analyze the empirical behavior of algorithms such as NSGA-II and SPEA2, which explicitly utilize the distribution properties of Pareto front approximations when parts of the Pareto front are restricted.

The following restrictions can be scaled easily in positions, size, and number. Here, infeasible areas in the objective space of dimension  $m$  are defined by  $m$ -dimensional spheres with radii  $r_j$  ( $j = 1, \dots, k$ ) and center points  $(c_{1j}, \dots, c_{mj})^T$ . The position and the radii of the spheres may change over time (see Fig. 1). With a value  $\varepsilon > 1$ , the center points depart from  $PF_{true}$ . Moving circular obstacles in the objective space is a new way to analyze the convergence robustness of the optimizing algorithms. The corresponding inequalities for the restrictions are:

$$g_j : r(t)^2 - (\varepsilon(t) \cdot c_{1j} - f_1(\mathbf{x}))^2 - \dots - (\varepsilon(t) \cdot c_{mj} - f_m(\mathbf{x}))^2 \leq 0, \quad j = 1, \dots, k \quad (4)$$

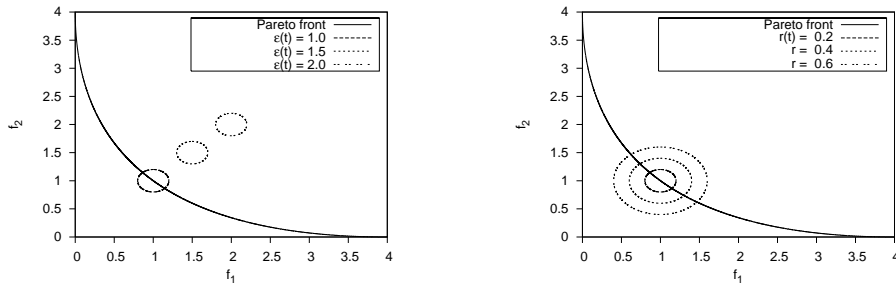


**Fig. 1.** Dynamic restrictions with varying position (left) or radii (right).

## 4 Multi-objective Evolutionary Algorithms

Today, NSGA-II [9] and SPEA2 [10] surely belong to the most commonly applied MOEA. The analysis of these algorithms implies a good comparability and applicability of the following results for many research fields that intend to allow dynamics in optimization problems. Variants of above algorithms for noisy optimization [11] have not been taken into account because the defined problems return exact values without any noise. Furthermore, the use of an archive may lead to better results with periodical dynamics.

Additionally, the MSOPS (Multiple Single Objective Pareto Sampling) [12] is analyzed to get an impression of the behavior of a stochastic population based algorithm that does not utilize the Pareto-dominance principle. MSOPS works with a weighted Min-Max aggregation of objectives and a ranking scheme due to multiple weight vectors called targets. In contrast to conventional linear aggregation approaches, weighted Min-Max is able to find solutions also for non-convex Pareto fronts. The multi-objective PISA library [13] served as a common interface to well tested genetic operators such as Simulated Binary Crossover (SBX) and Polynomial Mutation (PM) [15, page 109 et sqq.]. Differential Evolution (DE) variation operators DE1 and DE2 [14] were not provided by PISA and have been added by the authors. In PISA variation modules can be combined with many common selection modules like NSGA-II and SPEA2. MSOPS was not provided in PISA and has been added for a more comprehensive analysis.

## 5 Metrics

The quality of a Pareto front approximation  $\mathbf{PF}_{approx}$  is often measured by functions which assign a real value to evaluate the given  $\mathbf{PF}_{approx}$ . In the MOEA terminology these measures are called (unary) metrics<sup>4</sup>. The use of these functions allows to compare approximations of different MOEA and to analyze the progress in optimization. Most metrics focus on the distance to the Pareto front and/or the distribution of solutions. In order to analyze both aims separately, two metrics – a convergence and a distribution metric – are used.

The generational distance metric  $G_\tau$  was introduced by van Veldhuizen and Lamont. Given a set of discrete  $N$  solutions of a MOEA in generation  $\tau$ ,  $G_\tau$  is defined as follows [16, page 185]:

$$G_\tau := \frac{\sqrt{\sum_{i=1}^N d_i^2}}{N} \quad (5)$$

The  $d_i$  are the minimum euclidean distances of one discrete solution to an optimal solution. Here, this measure is calculated in decision space because for the most part of the problems considered the Pareto set is dynamically shifted.

---

<sup>4</sup> The strict mathematical definition of a real metric is not always guaranteed by MOEA-metrics.

Most distribution metrics calculate euclidean distances to evaluate the distribution of solutions. The shape and structure of the problem’s Pareto front is neglected. Path integrals offer the possibility to determine the distance between two discrete solutions via the length of the delimited path on the Pareto front. Thus, a new distribution metric – the *PL*-metric – is introduced. A precondition for the necessary calculations is an analytic closed description of  $\mathbf{PF}_{true}$ . This is true for the DSW as well as for the FDA1-3 functions.

A path between  $[a, b]$  can be defined by a continuous parametric function  $\gamma : [a, b] \subseteq \mathbb{R} \rightarrow \mathbb{R}^m$ ,  $\gamma(t) = (\gamma_1(t), \dots, \gamma_m(t))^T$ . For bi-objective problems with a continuous Pareto front  $f_2(f_1)$  the corresponding path follows  $\gamma(t) = (t, f_2(t))$ . Let  $\gamma$  be a path that is continuously differentiable in  $[a, b]$ . Then the length  $L(\gamma, a, b)$  of a path between  $[a, b]$  on  $\gamma$  is

$$L(\gamma, a, b) := \int_b^a |\dot{\gamma}| dt = \int_b^a \sqrt{\dot{\gamma}_1^2 + \dots + \dot{\gamma}_m^2} dt \quad (6)$$

where  $\dot{\gamma}$  is the derivative of  $\gamma$  in  $t$  and  $|\cdot|$  is the euclidean norm.

The *PL*-metric is defined by the the normalized product of the path between sorted neighboring points on  $\mathbf{PF}_{true}$ <sup>5</sup> adding 1 to ensure that new solutions increase the value of the metric:  $\xi_{x_i} = L(\gamma, \mathbf{f}(x_i), \mathbf{f}(x_{i+1})) + 1$ . Analytical proofs show that the *PL*-metric attains its unique maximum, if the path that describes  $\mathbf{PF}_{true}$  is divided into equidistant sections, i.e. a uniform approximation of  $\mathbf{PF}_{true}$  is found. In this case the measure reaches

$$\left(1 + \frac{L_{\mathbf{PF}_{true}}}{|\mathbf{PF}_{approx}| - 1}\right)^{|\mathbf{PF}_{approx}| - 1} \leq e^{L_{\mathbf{PF}_{true}}} \quad (7)$$

with equality for  $|\mathbf{PF}_{approx}| \rightarrow \infty$ . With this condition, the *PL*-metric can be numerically stable normalized in  $[0, 1]$  using the natural logarithm:

$$PL_\tau := \frac{\ln(\prod_{\mathbf{f}(x_i) \in \mathbf{PF}_{true}} \xi_{x_i})}{\ln e^{L_{\mathbf{PF}_{true}}}} = \frac{\sum_{\mathbf{f}(x_i) \in \mathbf{PF}_{true}} \ln(\xi_{x_i})}{L_{\mathbf{PF}_{true}}} \quad (8)$$

More than two objectives and disconnected Pareto fronts complicate the application of the *PL*-metric. Thus, in this cases Schott’s spacing metric [16, page 186] is used. For illustration purposes also the success ratio

$$SC_\tau = \frac{|\{\mathbf{x} | \mathbf{f}(\mathbf{x}) \in \mathbf{PF}_{true}\}|}{|\mathbf{PF}_{approx}|} \quad (9)$$

is computed.

---

<sup>5</sup> Due to the approximative character of MOEA, a solutions is said to be in  $\mathbf{PF}_{true}$ , if it is in an  $\varepsilon$ -region near  $\mathbf{PF}_{true}$ . In the analysis  $\varepsilon = 0.01$  is used.

**Table 1.** Setting for the Selection- and Variation Operators

| Selection | Parameter                | Setting  | Variation  | Parameter                    | Setting          |
|-----------|--------------------------|----------|------------|------------------------------|------------------|
| General   | $\alpha$ pop. size       | 100      | SBX        | $p_c$ crossover rate         | 0.5              |
|           | $\lambda$ parents        | 100      |            | $\eta_c$ spread factor       | 15               |
|           | $\mu$ offspring          | 100      | Uniform    | $p_{swap}$ prob.             | 0.5              |
|           | $\kappa$ age             | $\infty$ | Poly. Mut. | $p_m$ mutation rate          | $1/ \mathbf{x} $ |
|           | tournament               | binary   |            | $\eta_m$ perturbation factor | 20               |
| MSOPS     | $T$ target vectors       | 50       | DE1        | $F$ weight                   | 0.7              |
|           |                          |          |            | $CR$ insert prob.            | 0.5              |
| SPEA2     | $N$ archive size         | 100      | DE2        | $F$ weight                   | 0.85             |
|           |                          |          |            | $\lambda_{DE}$ weight        | 0.85             |
| NSGA-II   | no additional parameters |          |            | $CR$ insert prob.            | 1                |

## 6 Experimental Setup

The selection module MSOPS and the DE variation operators were implemented for PISA in C++. The metrics were calculated in MATLAB. Table 1 shows the parameter settings<sup>6</sup>. Each experiment was performed 20 times and the arithmetic mean was used to get an impression of the average system behavior. Extreme values occurring in single runs are neglected.

## 7 Empirical Results

The first class with static  $\mathbf{PF}_{true}$  and dynamic  $\mathbf{P}_{true}$  is analyzed with DSW1, DSW2, FDA1 and FDA4. In the beginning, the severity of change  $s$  is linearly increased. If SBX and PM are used, the results on the one-dimensional shifted sphere function DSW1 show similarities to the findings of Bäck [8]. Like the evolutionary strategy on the shifted single-objective sphere model, all MOEA considered are able to follow the moving optimum with a distance that is about quadratic in the currently applied  $s$ . Fig. 2 shows this behavior exemplary for NSGA-II. The perturbances in the graph for higher  $s$  are caused by changes in the shifting direction of the Pareto set to ensure that  $\mathbf{P}_{true}$  stays in the feasible set. Further experiments show that the distance to the Pareto set is approximately the same for the corresponding static value of  $s$ . Thus, the predictability of change has small influence on the MOEA.

The  $PL$ -metric shows a linearly decreasing trend (see Fig. 3) for increasing severity of change  $s$ . MSOPS tends to concentrate toward the center region of the Pareto front for small  $s$  which implicates lower values of  $PL_\tau$ .

The use of DE1 and DE2 results in worse values of both metrics. The populations collapse and the operators are no longer able to create new solutions<sup>7</sup>. Disconnected Pareto sets as in DSW2 delay the collapse of the population and

<sup>6</sup> The settings are chosen following suggestions of Deb et al. [9, 14, 15]

<sup>7</sup> DE operators create new solutions as weighted sums of current individuals. To determine the best individual, the relation defined in the concerned algorithm is used.

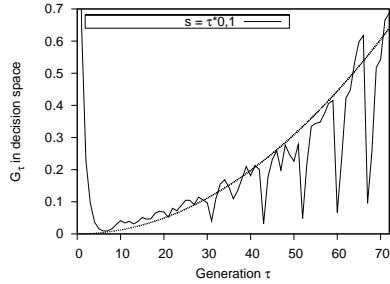


**Fig. 2.** The generational distance  $G_\tau$  of NSGA-II using SBX and PM on DSW1 with  $\tau_t = 1$  and linear increased  $s = \tau \cdot 0.1$ .

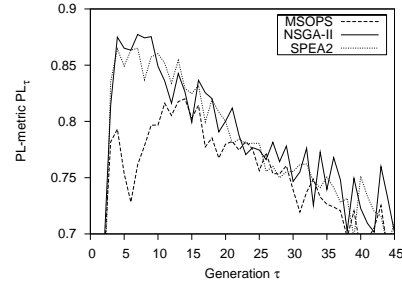


**Fig. 3.** The  $PL$ -metric  $PL_\tau$  of the considered selection algorithms using SBX and PM on DSW1 with  $\tau_t = 1$  and  $s = \tau \cdot 0.05$ .

improve the power of DE slightly, while the use of SBX and PM shows nearly same results on DSW1 and DSW2. All algorithms tend to concentrate soon at only one of the partitions of  $\mathbf{P}_{true}$ . This is sufficient to cover all parts of  $\mathbf{PF}_{true}$ .

The analysis of different change frequencies  $\tau_t^{-1}$  is performed on FDA1. The dimension of the decision space is raised to  $n = 20$  with  $s = 1/n_t = 0.1$ . The main focus is the ability of the MOEA to obtain advantages to a restart strategy which randomly reinitializes its solutions after every change. If  $\tau_t = 1$ , all algorithms fail to approximate  $\mathbf{P}_{true}$  permanently. Instead, a convergence to  $x_2, \dots, x_n = 0.5$  representing the center of the search space can be observed (see Fig. 4). The average distance over all generations is minimized. With increasing  $\tau_t$ , in the static phases the algorithms using SBX and PM succeed in converging toward  $\mathbf{P}_{true}$ . After 25 generations, i.e. 2500 function evaluations, the first solutions reach  $\mathbf{P}_{true}$ . Like Fig. 5 shows, NSGA-II converges faster than MSOPS which converges faster than SPEA2. All algorithms perform significantly better than the best restart strategy NSGA-II Re in regard to both metrics. Historically evolved solutions can be of use.

FDA4 is analyzed with three objectives and decreases the dimension of the decision space to  $n = 12$ . MSOPS can obviously improve the generational distance while NSGA-II and SPEA2 need much more function evaluations to reach  $\mathbf{PF}_{true}$  (see Fig. 5). This can be related to a decreasing selection pressure because of more incomparable solutions in regard to the dominance relation used in these algorithms. Again MSOPS tend to concentrate at certain spots of  $\mathbf{PF}_{true}$  while SPEA2 and NSGA-II reach good distributions.

Similar results can be observed in the analysis of the second class with growing Pareto fronts and strong modifications in the density of arguments such as FDA3 and FDA5. Whenever the population contains a lot of incomparable individuals the Pareto dominance based algorithms can not guarantee further convergence. If there are no density modifications as in DSW3, NSGA-II and SPEA2 succeed in approximating even large Pareto fronts regarding the  $PL$ -metric.



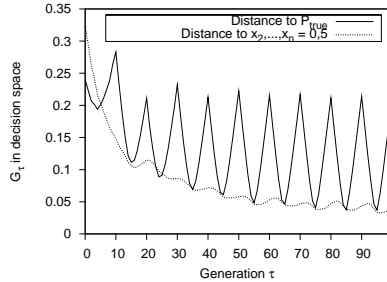


**Fig. 4.** The generational distance  $G_\tau$  of NSGA-II using SBX and PM on FDA1 with  $\tau_t = 1$  and  $s = 0.1$ . The distance to the static optimum of the average distance is also depicted.

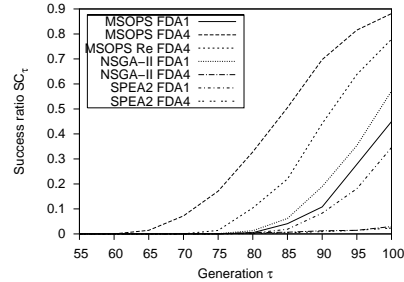


**Fig. 5.** The success ratio  $SC_\tau$  of the considered algorithms using SBX and PM on FDA1 and FDA4 with  $\tau_t = 50$  and  $s = 0.1$  in the second time step  $t = 1$ .

FDA2 and DTF with dynamically changing  $\psi$  are used to analyze the third class of changing  $\mathbf{PF}_{true}$  and static  $\mathbf{P}_{true}$ . First, all algorithms successfully converge to  $\mathbf{PF}_{true}$ . After that, the changes in shape (FDA2) and structure (DTF) of the Pareto front induce short declines in both metrics. MSOPS reveals problems in adapting the population to new shapes and structures. This shows that even changes with no influence on the optimal solutions can present a challenge to MOEA. NSGA-II performs best in adapting to the new shapes of  $\mathbf{PF}_{true}$  while SPEA2 shows advantages in approximating new structures regarding the PL-metric. A dynamic structure of the function describing  $\mathbf{PF}_{true}$  (DTF) and structural changes due to dynamic restrictions show the same effects.

The analysis of the last class using DTF with dynamic  $\omega$  indicates that dynamic changes not always enhance the difficulty of a given problem. Shifting local optima assists MOEA to leave local attractors and to converge to the static global optima.

## 8 Summary and Outlook

An extensive empirical analysis is performed on standard benchmark functions as well as on new designed functions for previously uncovered problem cases in dynamic multi-objective optimization. A new metric is introduced to face the problem that most distribution metrics do not include informations about shape and structure of the Pareto front.

The basic DE operators are only applicable to low-dimensional decision spaces. For complex problems, extensions are necessary to avoid the problem of preliminary convergence. Whenever a problem produces a lot of incomparable solutions in regard to the dominance relation, alternative MOEA like MSOPS show advantageous behavior.

A statistical search for the best parameter settings as well as the analysis of the population structure of the MOEA is matter for future research.

## 9 Acknowledgment

The research projects B12, C12, and T3 are supported by the German Research Foundation (DFG) as projects in the collaborative research center SFB 531 at the University of Dortmund, Germany.

## References

1. Y. Jin, B. Sendhoff: Constructing dynamic optimization test problems using the multi-objective optimization concept. In: Proceedings of the EvoWorkshops 2004. Springer (2004), 525–536
2. M. Farina, K. Deb, and P. Amato: Dynamic multiobjective optimization problems: Test cases, approximation, and applications. In: Proceedings of Evolutionary Multi-Criterion Optimization 2003. Springer (2003), 311–326
3. M. Farina, K. Deb, and P. Amato: Dynamic multiobjective optimization problems: Test cases, approximations, and applications. IEEE Transactions on Evolutionary Computation. 8(2004)5, 425–442
4. K. Deb: Multi-objective genetic algorithms: Problem difficulties and construction of test problems. Evolutionary Computation. 7(1999)3, 205–230
5. K. Deb, L. Thiele, M. Laumanns, and E. Zitzler: Scalable multi-objective optimization test problems. In: Proceedings of the Congress on Evolutionary Computation 2002. IEEE (2002), 825–830
6. J. Branke: Evolutionary Optimization in Dynamic Environments. Kluwer, Boston, MA, 2002
7. J. D. Schaffer: Multiple objective optimization with vector evaluated genetic algorithms. In: Proceedings of the first International Conference on Genetic Algorithms. Lawrence Erlbaum Ass. (1985), 93–100
8. T. Bäck: On the behavior of evolutionary algorithms in dynamic environments. In: Proceedings of the second World Congress on Computational Intelligence. IEEE (1998), 446–451
9. K. Deb, S. Agrawal, A. Pratap, and T. Meyarivan: A Fast Elitist Non-dominated Sorting Genetic Algorithm for multi-objective optimisation: NSGA-II. In: Proceedings of Parallel Problem Solving from Nature VI. Springer (2000), 849–858
10. E. Zitzler, M. Laumanns, and L. Thiele: SPEA2: Improving the Strength Pareto Evolutionary Algorithm for multiobjective optimization. In: Proceedings of the EUROGEN 2001 Conference. CIMNE (2002), 95–100
11. J. Teich: Pareto-Front exploration with uncertain objectives. In: Proceedings of Evolutionary Multi-Criterion Optimization 2001. Springer (2001), 314–328
12. E. Hughes: Multiple single objective Pareto sampling. In: Proceedings of the Congress on Evolutionary Computation 2003. IEEE (2003), 2678–2684
13. St. Bleuler, M. Laumanns, L. Thiele, and E. Zitzler: PISA – A Platform and programming language independent Interface for Search Algorithms. In: Proceedings of Evolutionary Multi-Criterion Optimization 2003. Springer (2003), 494–508
14. R. Storn, K. Price: Differential Evolution – A simple and efficient adaptive scheme for global optimization over continuous spaces. Technical Report No. 95-012. International Computer Science Institute, 1947 Center Street, Berkeley, CA (1995)
15. K. Deb: Multi-objective Optimization using Evolutionary Algorithms. Wiley, Chichester, UK, 2001
16. Y. Collette, P. Siarry: Multiobjective Optimization. Springer, Berlin, 2003